HAL
open science

The N-terminal Domain of Hepatocyte Growth Factor Inhibits the Angiogenic Behavior of Endothelial Cells Independently from Binding to the c-met Receptor

Tatyana Merkulova-Rainon, Patrick England, Shunli Ding, Corinne Demerens, Gérard Tobelem

To cite this version:

Tatyana Merkulova-Rainon, Patrick England, Shunli Ding, Corinne Demerens, Gérard Tobelem. The N-terminal Domain of Hepatocyte Growth Factor Inhibits the Angiogenic Behavior of Endothelial Cells Independently from Binding to the c-met Receptor. Journal of Biological Chemistry, 2003, 278 (39), pp.37400 - 37408. 10.1074/jbc.m212768200 . pasteur-03525665

HAL Id: pasteur-03525665

https://pasteur.hal.science/pasteur-03525665v1

Submitted on 14 Jan 2022

HAL is a multi-disciplinary open access archive for the deposit and dissemination of scientific research documents, whether they are published or not. The documents may come from teaching and research institutions in France or abroad, or from public or private research centers.

L'archive ouverte pluridisciplinaire **HAL**, est destinée au dépôt et à la diffusion de documents scientifiques de niveau recherche, publiés ou non, émanant des établissements d'enseignement et de recherche français ou étrangers, des laboratoires publics ou privés.

Distributed under a Creative Commons Attribution 4.0 International License

THE JOURNAL OF BIOLOGICAL CHEMISTRY
Vol. 278, No. 39, Issue of September 26, pp. 37400–37408, 2003
Printed in U.S.A.
© 2003 by The American Society for Biochemistry and Molecular Biology, Inc.

The N-terminal Domain of Hepatocyte Growth Factor Inhibits the Angiogenic Behavior of Endothelial Cells Independently from Binding to the c-met Receptor*

Received for publication, December 16, 2002, and in revised form, May 30, 2003
Published, JBC Papers in Press, July 7, 2003, DOI 10.1074/jbc.M212768200

Tatyana Merkulova-Rainon‡§, Patrick England¶, Shunli Ding‡‖, Corinne Demerens‡, and Gérard Tobelem‡

From the ‡Institut des Vaisseaux et du Sang, Centre de Recherche de l'Association Claude Bernard, Hôpital Lariboisière, 8 rue Guy Patin, 75475, Paris Cedex 10 and the ¶Plate-forme de Biophysique des Macromolécules et de leurs Interactions, Institut Pasteur, 28, rue du Docteur Roux, 75724 Paris Cedex 15, France

Hepatocyte growth factor (HGF) is a pleiotropic factor that plays an important role in complex biological processes such as embryogenesis, tissue regeneration, cancerogenesis, and angiogenesis. HGF promotes cell proliferation, survival, motility, and morphogenesis through binding to its receptor, a transmembrane tyrosine kinase encoded by the *MET* proto-oncogene (c-met). Structurally speaking, HGF is a polypeptide related to the enzymes of the blood coagulation cascade. Thus, it comprises kringle domains that in some other proteins have been shown to be responsible for the anti-angiogenic activity. To check whether the isolated kringles of HGF were able to inhibit angiogenesis, we produced them as recombinant proteins and compared their biological activity with that of the recombinant HGF N-terminal domain (N). We showed that (i) none of the isolated HGF kringle exhibits an anti-angiogenic activity; (ii) N is a new anti-angiogenic polypeptide; (iii) the inhibitory action of N is not specific toward HGF, because it antagonized the angiogenic activity of other growth factors, such as fibroblast growth factor-2 and vascular endothelial growth factor; and (iv) in contrast with full-length HGF, N does not bind to the c-met receptor *in vitro*, but fully retains its heparin-binding capacity. Our results suggest that N inhibits angiogenesis not by disrupting the HGF/c-met interaction but rather by interfering with the endothelial glycosaminoglycans, which are the secondary binding sites of HGF.

The hepatocyte growth factor (HGF)[1] (1), also known as Scatter factor (2), was originally described as a potent mitogen for mature hepatocytes and as a cytokine capable of inducing the dissociation (scattering) of epithelial cells. HGF has now been proven to be a pleiotropic factor that acts on a wide array of target cell types, including epithelial, endothelial, neuronal, and hematopoietic cells (3). HGF promotes cell proliferation, survival, motility, and morphogenesis through binding to its receptor, a transmembrane tyrosine kinase encoded by the *MET* proto-oncogene (c-met) (4, 5). The signaling cascade triggered by the binding of HGF to c-met contributes to complex biological processes, such as embryogenesis, tissue regeneration, and cancerogenesis (3, 6). Studies performed in the recent years have shown that HGF is also a potent angiogenic molecule (7–10).

HGF is a polypeptide structurally related to the enzymes of the blood coagulation cascade. In the cell it is synthesized as a biologically inactive single chain precursor that is then cleaved by specific serine proteases yielding a fully active disulfide-linked heterodimer composed of α- and β-chains (11, 12). The α-chain consists of an N-terminal domain (N) followed by four kringle modules and mediates the binding of HGF to the c-met receptor (13, 14). Additional structure-function studies indicated that the N-terminal domain and first kringle (K1) are primarily involved in this interaction (15). The α-chain is also involved in the high affinity binding of HGF to heparin. Based on deletion analysis, the hairpin loop in the N-terminal domain and the second kringle (K2) were shown to be implicated in heparin binding (16, 17). Recently x-ray crystal structures were determined for the complexes of heparin with NK1, a naturally occurring HGF variant containing N domain and K1, which suggested that some heparin binding activity is also located within K1 (18). Up to date, no discernible function has been demonstrated for the third (K3) and fourth (K4) kringles of HGF.

The kringle domain is an 80-amino acid triple-loop structure maintained by three intramolecular disulfide bonds highly conserved between different kringle containing proteins (19). Kringles are thought to play an important role in regulating the nature and strength of protein-protein interactions. Several reports have documented the anti-angiogenic activity of isolated kringles of different origin. The most known example is angiostatin, the three- to four-kringle containing fragment of human plasminogen (20, 21), and plasminogen kringle 5 (22). More recently the prothrombin kringle-2 domain has been

* This work was supported in part by grants from the Ligue Nationale Contre le Cancer and from the Association pour la Recherche sur le Cancer (to G. T.). The costs of publication of this article were defrayed in part by the payment of page charges. This article must therefore be hereby marked "*advertisement*" in accordance with 18 U.S.C. Section 1734 solely to indicate this fact.

§ To whom correspondence should be addressed: Tel.: 33-1-45-26-21-98; Fax: 33-1-42-82-94-73; E-mail: tatiana.merkoulova-rainon@lrb.ap-hop-paris.fr.

‖ Recipient of a fellowship from the Association Franco-Chinoise pour la Recherche Scientifique & Technique.

[1] The abbreviations used are: HGF, hepatocyte growth factor; N, N-terminal domain of HGF; K1, K2, K3, K4, the first, second, third, and fourth kringles of HGF, respectively; NK1, an HGF variant containing N domain and K1; NK2, an HGF variant containing N domain and the first two kringles; IPTG, isopropyl β-D-1-thiogalactopyranoside; NF heparin, non-fractionated heparin; LMW, low molecular weight; NHS, normal human serum; FBS, fetal bovine serum; FGF-2, fibroblast growth factor 2; VEGF, vascular endothelial growth factor; PDGF BB, platelet-derived growth factor BB; c-met/Fc, chimerical protein composed of the HGF receptor (c-met) extracellular domain fused to human IgG_1 Fc; HUVEC, human umbilical vein endothelial cell; hASMC, human aortic smooth muscle cell; NHEK, human normal epidermal keratinocyte; SPR, surface plasmon resonance; GAG, glycosaminoglycan; PBS, phosphate-buffered saline.

This paper is available on line at http://www.jbc.org

This is an Open Access article under the CC BY license.

shown to inhibit endothelial cell growth and angiogenesis in the chorioallantoic membrane of chick embryos (23); a recombinant apolipoprotein (a) containing 18 kringle repeats has been implicated in the reduction of tumor microvessel density in transgenic mice (24). The molecular mechanism by which the kringles suppress blood vessel formation is still unknown. We hypothesized that one or more of the kringles of HGF might inhibit angiogenesis and that the mechanism of the anti-angiogenic activity of a kringle domain could be related to its ability to antagonize the HGF binding to c-met. To verify this hypothesis, we produced each of the five HGF α-chain individual modules as recombinant proteins and analyzed their binding properties and biological activity in different assays related to angiogenesis.

EXPERIMENTAL PROCEDURES

Materials—The bacterial expression vectors pET15b and pET21b(+), the *Escherichia coli* expression strain BL21(DE3), and tetracycline hydrochloride were purchased from Novagen (VWR International, Fontenay-sous-Bois, France).

EZMix 2×YT microbial medium, carbenicillin, chloramphenicol, IPTG, non-fractionated heparin (catalog number H 3393) and low molecular weight heparin (average molecular weight 3000, catalog number H 3400), a peroxidase conjugated antibody against goat IgG, protein A from *Staphylococcus aureus*, and 0.2% gelatin were all purchased from Sigma (St. Louis, MO). *Pwo* DNA polymerase was purchased from Roche Diagnostics (Mannheim, Germany). TALON Superflow metal affinity resin was obtained from Clontech (Palo Alto, CA). The Ultrafree-4 and Ultrafree-15 Centrifugal Filter Device supplied with Bio-Max-5K filters and 0.22-μM Millex-GV filter units were obtained from Millipore (Bedford, MA). The BCA protein assay reagent, the IODO-GEN Pre-Coated Iodination Tubes, and EZ-Link biotin-LC-hydrazide were all obtained from Pierce (Perbio Sciences, Bezons, France). Nitrocellulose Hybond C Extra membranes, ECL Plus Western blotting detection reagent, Sephadex G-25M prepacked PD-10 columns, and [*methyl*-^{3}H]thymidine (74 GBq/mmol) were all purchased from Amersham Biosciences (Buckinghamshire, UK). Iodine-125 (3.7 GBq/ml) was purchased from ICN Biomedicals (Costa Mesa, CA).

All cell culture reagents were purchased from Invitrogen (Cergy Pontoise, France) unless otherwise specified. Normal human AB male serum (NHS) and fetal bovine serum (FBS) were obtained from BioWest (Cholet, France). NSO-expressed recombinant human HGF, recombinant human FGF-2, $VEGF_{165}$, $VEGF_{121}$, PDGF BB, c-met/Fc chimera (soluble c-met), and human HGF-specific polyclonal goat IgG were all purchased from R&D Systems (Minneapolis, MN). Type I rat tail collagen was purchased from BD Biosciences (Bedford, MA). Research grade CM5 sensor chips (carboxymethylated dextran matrix), SA sensor chips, amine coupling kit (1-ethyl-3-(3-dimethylaminopropyl)carbodiimide/*N*-hydroxysuccinimide), and surfactant P20 were all obtained from BIACORE (Uppsala, Sweden).

Recombinant Protein Expression and Purification—The isolated HGF α-chain domains were produced using the pET-based bacterial expression system (Novagen). The DNA encoding different HGF polypeptides was generated by PCR using *Pwo* DNA polymerase and the pGEM/HGF-TM construct as a template (a generous gift of Dr. Pascale Briand at Institut Cochin de Génétique Moléculaire) (25). This construct encodes for an HGF splice variant lacking a pentapeptide FLPSS in the first kringle domain (the amino acids from 162 to 166, according to the sequence deposited in the Swiss-Prot data base under accession number P14210) but which preserves all the biological activity of full-length variant (26, 27). The primers used for PCR were: N forward, 5′-ATATCATATGCAAAGGAAAAGAAGAAATACAA-3′ and N reverse, 5′-ATATGGATCCTAGTTTCTAATGTAGTCTTTGTTTT-3′; K1 forward, 5′-ATATCATATGAACTGCATCATTGGTAAAGGA-3′ and K1 reverse, 5′-ATATGTCGACTTCTGAACACTGAGGAATGTC-3′; K2 forward, 5′-ATATGGATCCAGTTGAATGCATGACCTGCA-3′ and K2 reverse, 5′-ATATGTCGACGTCAGCGCATGTTTTAATTGC-3′; K3 forward, 5′-ATATGGATCCAACTGAATGCATCCAAGGTC-3′ and K3 reverse, 5′-ATATGTCGACCATATCACAGTTTGGAATTTG-3′; and K4 forward, 5′-ATATGGATCCAGATTGTTATCGTGGGAATGG-3′ and K4 reverse, 5′-ATATGTCGACACCTTCACAACGAGAAATAGG-3′. The purified PCR fragment encoding the HGF N-terminal domain (amino acids from 32 to 127) was cloned into *Nde*I and *Bam*HI sites of pET15b, in-frame with N-terminal His Tag. The DNA for K1 (amino acids from 127 to 208) was cloned into *Nde*I and *Sal*I sites of pET21b(+), in-frame with C-terminal His Tag, and the DNA for K2 (amino acids from 209 to 290), K3 (amino acids from 303 to 385), and K4 (amino acids from 390 to 471) were all cloned into *Bam*HI and *Sal*I sites of pET21b(+), in-frame with N-terminal T7 Tag and C-terminal His Tag. All PCR-generated constructs were checked for polymerase fidelity by sequencing (Génome Express, Grenoble, France).

All plasmids encoding HGF kringles, or the plasmid encoding the HGF N domain were electroporated, respectively, into *E. coli* strain BL21(DE3), or into *E. coli* BL21(DE3) based strain pRI (kindly provided by Dr. Janne L. Simonsen at Arhus University) carrying two additional plasmids: one encoding a $tRNA^{Ile}$ specific for the rare isoleucine codon AUA and another for the LacZ repressor RP4. Bacteria were grown at 30 °C in EZMix 2× YT medium containing 1 M glucose and appropriate antibiotics. Protein expression was induced with 1 mM IPTG for 4 h at 25 °C. Bacterial cells were harvested by centrifugation and stored at −20 °C.

Bacterial pellets (5 g wet weight) were resuspended in 100 ml of lysis buffer (50 mM Tris-HCl, pH 7.4, containing 0.2 M NaCl, 10 mM imidazole, 10% glycerol, 1% Nonidet P-40, 2 mM β-mercaptoethanol, 1 mM phenylmethylsulfonyl fluoride, and 0.2 mg/ml lysozyme) and incubated for 20 min at room temperature with rotation. The suspensions were sonicated and centrifuged at 10,000 × *g* for 30 min. All HGF kringles were recovered in the supernatants and purified by cobalt-chelate affinity chromatography on a 2-ml TALON column under non-denaturing conditions. The pellet containing insoluble N was resuspended in 30 ml of isolation buffer (20 mM Tris-HCl, pH 8, containing 0.5 M NaCl, 2 M urea, and 2% Triton X-100) and subjected to three successive rounds of brief sonication, centrifugation (10,000 × *g* for 10 min), and resuspension. The supernatants from all three steps were pooled and applied to a TALON column equilibrated with isolation buffer. To achieve the N domain renaturation, the column was washed with a 2 to 0 M gradient of urea in IMAC buffer (20 mM Tris-HCl, pH 8, and 0.5 M NaCl) containing 10 mM imidazole. Renatured N was eluted by IMAC buffer containing 0.5 M imidazole.

Further steps were all performed at 4 °C. Selected column fractions corresponding to the peaks of purified N, K1, K2, K3, or K4 were pooled and diluted with 10 volumes of refolding buffer (PBS containing 10% glycerol, 1 mM reduced glutathione, and 0.2 mM oxidized glutathione). Following an overnight incubation with stirring, the protein solutions were concentrated using Ultrafree-15 Centrifugal Filter Devices and dialyzed against PBS containing 10% glycerol for 2 days with at least three changes of buffer. The final protein preparations were sterilized using 0.22-μM Millex-GV filter units and stored at −80 °C until required. The protein concentration was determined using the BCA protein assay. The purified recombinant HGF-derived proteins were analyzed by SDS-PAGE and by circular dichroism as described previously (28).

Cells—Human umbilical vein endothelial cells (HUVECs) were isolated by collagenase (Roche Diagnostics) digestion (29). Cells were routinely grown in flasks coated with gelatin, in M199 medium containing 2 mM glutamine, 50 units/ml penicillin, 50 μg/ml streptomycin, 2.5 μg/ml amphotericin B, 7.5% NHS, and 7.5% FBS (regular medium). HUVECs from the second or third passage were used. The human colorectal carcinoma cell line DLD-1, the human osteogenic sarcoma cell line TE 85, and the human pancreatic adenocarcinoma cell line Capan-1 were obtained from the American Type Culture Collection and were cultured in RPMI supplemented with 10% FBS. Human aortic smooth muscle cells (hASMCs) and the corresponding growth medium (SmGM-2), and the human normal epidermal keratinocytes (NHEK) and the corresponding growth medium (KGM) were purchased from Clonetics (BioWhittaker France).

Proliferation Assay—Cells that had been grown until confluence were harvested by trypsinization, and their proliferation was measured by use of a [^{3}H]thymidine incorporation assay. Cells were plated in 24-well plates: HUVECs at a density of 2×10^4 cells/well in M199 medium supplemented with 2.5% FBS, hASMCs at a density of 2×10^4 cells/well in SmGM-2 supplemented with 1% FBS, NHEKs at a density of 10^4 cells/well in KGM supplemented with 3 mg/ml AlbuMAX (Invitrogen), TE 85 cells at a density 5×10^3 cells/well, DLD-1 and Capan-1 cells at a density of 10^4 cells/well in RPMI supplemented with 3 mg/ml AlbuMAX. Cells were allowed to attach for 4 h at 37 °C, and proliferation was induced by adding 10% FBS or 10 ng/ml of FGF-2, $VEGF_{165}$, HGF, or PDGF BB. The rising concentrations (10–5000 nM) of purified recombinant HGF-derived proteins were added to some wells, and HUVECs were incubated for a further 24 h. [^{3}H]Thymidine (1 μCi/well) was added during the last 18 h of incubation. Cells were washed three times with PBS and treated with ice-cold 10% (w/v) trichloroacetic acid for 30 min. The resulting precipitates were solubilized with 0.3 N NaOH (0.5 ml/well),

and the incorporated radioactivity was measured in a LS-6500 multipurpose scintillation counter (Beckman Coulter, Fullerton, CA).

Migration Assay—HUVEC migration was evaluated in a modified Boyden chamber assay. Transwell cell culture chamber inserts (BD Biosciences) with porous polycarbonate filters (8-μM pore size) were coated with 0.2% gelatin in PBS. HUVECs suspended in M199 medium supplemented with 2.5% FBS were added to the inserts at 4×10^4 cells per well. The inserts were placed over chambers containing a chemotactic stimulus (10 ng/ml HGF, FGF-2, or $VEGF_{165}$), and cells were allowed to migrate for 5 h at 37 °C in a CO_2 incubator. For inhibition experiments one of the purified HGF α-chain-derived polypeptides (each at 1 μM) was added to the lower chamber. The filters were then rinsed with PBS, fixed with 1% (w/v) paraformaldehyde, and stained with hematoxylin of Harris. The upper surface of the filters was scraped with a cotton swab to remove the non-migrant cells. The number of cells per high power field (×200) was recorded. Each experimental point was performed in triplicate, and 10 fields per filter were analyzed.

"In Gel" Three-dimensional Collagen Culture—Type I rat tail collagen composed gels were formed according to the manufacturer's recommendations. Briefly, an ice-cold collagen solution was neutralized by addition of 1 N NaOH and mixed with 10× PBS in the ratio 9:1. HUVECs (passage 2) isolated by trypsin-EDTA treatment and suspended in the M199 medium supplemented with 2.5% FBS, were added at a final concentration of 5×10^5 cells/ml in a 1 mg/ml collagen solution. 0.4 ml of this suspension was poured into wells of a 24-well plate (Nunc, Roskilde, Denmark), and the gels were allowed to form at 37 °C for 40 min. The gels were then overlaid with 0.5 ml of M199 medium supplemented with 2.5% fetal bovine serum and 10 ng/ml of the growth factors. When indicated, purified recombinant HGF domains (1 μM) were added at the same time as the growth factors to the overlaying medium. Cultures were incubated for 48 h at 37 °C in a humidified atmosphere containing 5% CO_2. Digital images were captured using a Kappa CF11DSP charge-coupled device camera (KAPPA opto-electronics GmbH, Gleichen, Germany).

Radiolabeled Ligand Binding and Displacement Experiments—HGF (5 μg), $VEGF_{165}$ (10 μg), FGF-2 (10 μg), or recombinant HGF N-terminal domain (25 μg) were iodinated with 1 mCi of [^{125}I]NaI using the IODO-GEN Pre-Coated Iodination Tubes according to the manufacturer's instructions. Iodinated proteins were purified by chromatography on PD-10 columns equilibrated with 25 mM Tris-HCl, pH 7.4, containing 0.4 M NaCl, 5 mM EDTA, and 0.25% AlbuMAX and concentrated using the Ultrafree-4 Centrifugal Filter Device. The specific activities determined by trichloroacetic acid precipitation were 18×10^6 cpm/pmol for ^{125}I-HGF, 8×10^6 cpm/pmol for ^{125}I-$VEGF_{165}$, 9×10^5 cpm/pmol for ^{125}I-FGF-2, and 5×10^5 cpm/pmol for ^{125}I-N.

Binding and displacement studies with the iodinated proteins were carried out on confluent HUVECs in 24-well dishes, at 4 °C. Cells were washed with PBS and preincubated for 30 min with 0.5 ml of binding medium (M199 medium containing 0.1% AlbuMAX). To determine the binding parameters for N, increasing amounts of radiolabeled N were added to HUVECs, with or without a 100-fold molar excess of unlabeled N, and incubated for 6 h. For displacement experiments, constant amounts of radiolabeled HGF (1.5 nM), $VEGF_{165}$ (1.2 nM), or FGF-2 (1 nM) were added to HUVECs in the presence of increasing concentrations of unlabeled N for 4 h. At the end of incubation, cells were washed three times with binding medium and solubilized with 0.3 N NaOH. HUVEC-associated radioactivity was determined in a γ-counter, and the results were analyzed using the program Ligand included in the KELL package (Biosoft, Cambridge, UK). All experiments were done in triplicate. The K_d values represent the means ± S.D. obtained from three or four experiments.

In Vitro Binding Studies by Surface Plasmon Resonance—The binding studies were performed on a BIACORE 2000 instrument. The analytes were routinely diluted in BIACORE running buffer (PBS, pH 7.5, containing 0.005% P-20) completed with 0.2 mg/ml BSA, and injected at 20 μl/min. Between binding cycles the coated surfaces were regenerated by two injections of 1 M NaCl. In each case the first flow channel of the sensor chip did not contain any immobilized ligand and served as a reference surface. In one set of experiments, a non-fractionated heparin (NF heparin) was biotinylated with EZ-Link Biotin-LC-Hydrazide as described in a previous study (30) and about 600 RU were captured on the surface of streptavidin-coated SA sensor chips. The c-met/Fc chimera was captured on the surface of a CM5 sensor chip with immobilized protein A (600 RU). HGF and purified HGF domains were injected over immobilized heparin and c-met. In a second set of experiments, HGF and its domains were immobilized on the CM5 sensor chip surface (~1000 RU) using the amine coupling kit according to the manufacturer's instructions. NF heparin, low molecular weight heparin (LMW heparin), and soluble c-met, were used as analytes. Binding curves were obtained over a range of analyte concentrations for each of the analyte/ligand pairs. The data were analyzed with the non-linear least squares algorithm implemented in the BIAevaluation 3.1 software package.

Statistics—Results were expressed as mean ± S.E. Statistical significance was evaluated by analysis of variance followed by Bonferroni/Dunn analysis.

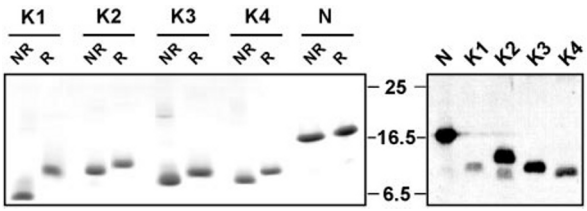

FIG. 1. **SDS-PAGE analysis of pure recombinant HGF α-chain domains.** 1 μg of protein per lane was resolved by 15% SDS-PAGE. *Left*, Coomassie Blue staining; samples were analyzed under either non-reducing (*NR*) or reducing (*R*) conditions. *Right*, Western blotting with anti-HGF antibodies.

RESULTS

Production and Purification of Recombinant HGF α-Chain Structural Modules—The HGF kringles were all expressed in *E. coli* in a soluble form. Recombinant N-terminal domain was mainly accumulated in insoluble inclusion bodies and was easily solubilized with 2 M urea containing 2% Triton X-100. The proteins were purified to homogeneity using a simple one-step procedure on TALON metal affinity column (Fig. 1). They were subsequently subjected to oxidative folding using the glutathione-based oxido-shuffling system. The final protein preparations were analyzed in SDS-PAGE under reducing and non-reducing conditions to ensure the presence of disulfide bonds (Fig. 1). We observed very little or no difference in the mobility of the non-reduced and reduced N, although this protein possesses two disulfide bonds. In contrast, the non-reduced K1 exhibited a substantial mobility shift compared with the reduced sample. Similar results had been previously reported for N and K1 produced in *E. coli* (31). K2, K3, and K4 also demonstrated an increased mobility under non-reducing conditions. These results indicate that our HGF kringle preparations have a compact conformation under non-reducing conditions and that the disulfide bonds were formed during the refolding procedure.

The circular dichroism analysis of N, K1, K2, K3, and K4 demonstrated that these proteins were folded. The far-UV CD spectra (180–260 nm) of N, K1, K2, K3, and K4 are all indicative of a high content in secondary structure. A broad band of positive ellipticity can be seen in the 230- to 260-nm region: it most probably originates from oxidized disulfides and aromatic residues involved in the characteristic hydrophobic core of the kringle-type folding. The near-UV CD spectra (240–340 nm) show bands in the 275- to 290-nm region, which are characteristic of an asymmetric orientation of aromatic residues (Trp and Tyr). These signals are typical for the folded tertiary structure of globular proteins (data not shown).

Effect of Isolated HGF Domains on Cell Proliferation—Angiogenic response involves a surge in endothelial cell proliferation, which could be induced by several growth factors (32). Under our experimental conditions, the highest capacity of induction of HUVEC proliferation was demonstrated for FGF-2, whereas HGF was a very poor mitogen (about 750% stimulation against 25%; Fig. 2, *A* and *B*, respectively). Therefore, we first analyzed the effect of isolated HGF domains on the proliferation of HUVECs stimulated with 10 ng/ml FGF-2 (Fig. 2*A*). In these experiments none of HGF-derived kringles exhibited any activity, whereas N inhibited HUVEC prolifera-

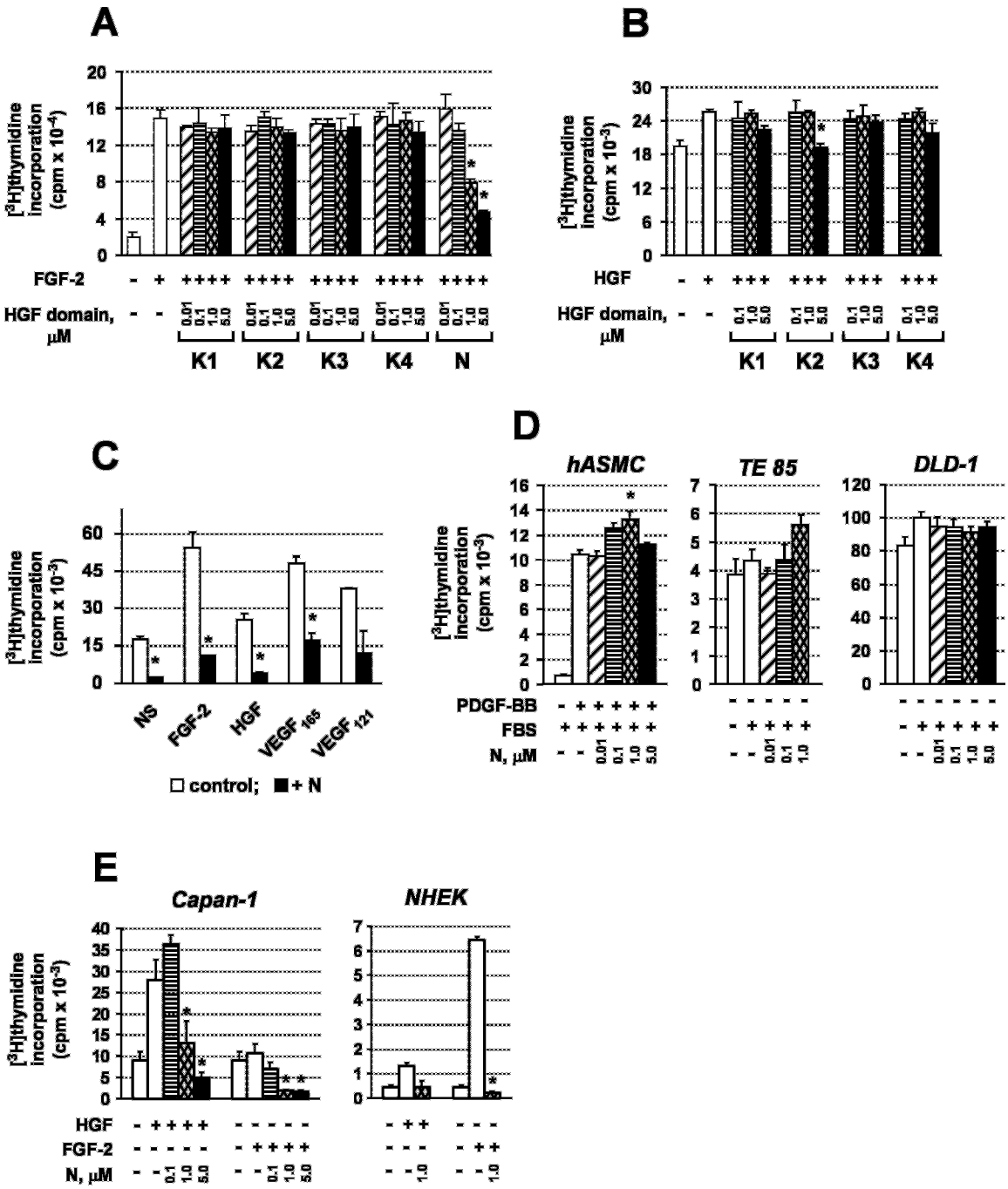

FIG. 2. **The N-terminal domain of human HGF inhibits HUVEC proliferation.** Growth-arrested HUVECs were stimulated with 10 ng/ml of FGF-2 (*A*), or 10 ng/ml of HGF (*B*) for 24 h in the presence of increasing concentration of purified N, K1, K2, K3, or K4. *C*, HUVECs were stimulated with 10 ng/ml FGF-2, HGF, $VEGF_{165}$, or $VEGF_{121}$ in the absence or in the presence of 3.7 μM N. *D*, hASMCs were stimulated with 10 ng/ml PDGF BB in the presence of 1% FBS; TE 85 or DLD-1 cells were stimulated with 10% FBS; *E*, NHEKs or Capan-1 were stimulated with 10 ng/ml HGF or 10 ng/ml FGF-2 in the presence of increasing concentrations of N. The mitogenic response was accessed by [^{3}H]thymidine incorporation. Values on the *y*-axis are the mean c.p.m. obtained from triplicate cultures. *NS*, unstimulated control. *, difference (*versus* stimulated control) is significant with 95% confidence. Results shown are representative of three or more experiments.

tion in a concentration-dependent manner. The influence of N on HUVEC proliferation could be detected at a concentration of 100 nM (about 10% of inhibition). Depending on the umbilical cord specimen, a maximum inhibition effect (up to 100%) was observed for a concentration of N of 1–5 μM.

Because our hypothesis was that kringles could modulate angiogenesis by competitive binding to the c-met receptor, we also studied the effect of recombinant HGF domains on the proliferation of HUVECs induced by HGF. The kringles of HGF had no effect on the proliferation of HUVECs in the presence of HGF (Fig. 2*B*). In contrast, N significantly inhibited the proliferation of HUVECs induced not only by HGF but also by two isoforms of VEGF: $VEGF_{165}$ and $VEGF_{121}$ (Fig. 2*C*). Thus, the anti-proliferative effect of N was not specific toward HGF.

We further tested the specificity of the anti-proliferative effect of N toward the endothelial cell type. In the preliminary experiments we showed that HGF was unable to stimulate the proliferation of hASM cells. In contrast, hASMC responded to PDGF BB (Fig. 2*D*), whereas PDGF BB had no effect on the proliferation of HUVECs (data not shown). The TE 85 and DLD-1 tumor cells did not respond to any of the growth factors tested in this study, and only DLD-1 cells could be slightly

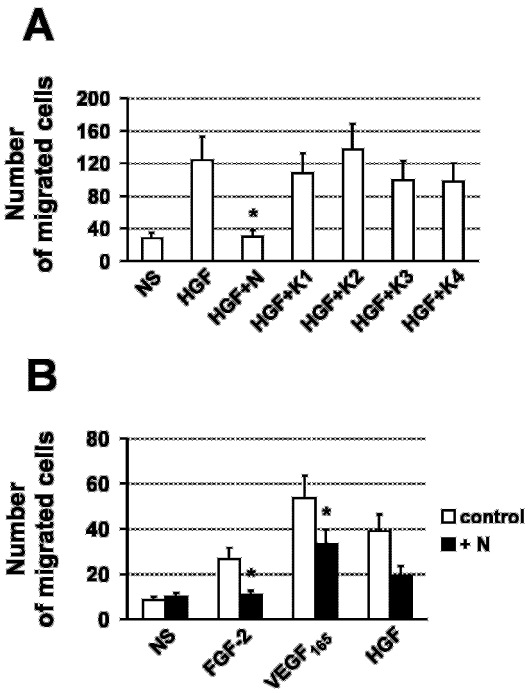

FIG. 3. **The N-terminal domain of human HGF inhibits HUVEC migration.** HUVEC migration in Transwell assay toward (*A*) 10 ng/ml HGF alone or HGF and one of purified HGF α-chain-derived polypeptides (5 μM). *B*, lower chamber contained 10 ng/ml FGF-2, $VEGF_{165}$, or HGF with or without 3.7 μM N. *NS*, unstimulated control. *, difference (*versus* stimulated control) is significant with 95% confidence. Results shown are representative of four independent experiments.

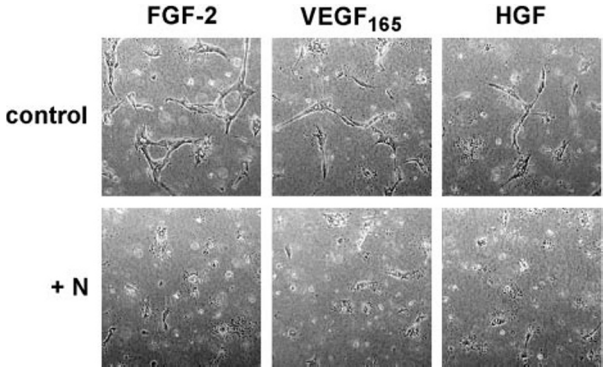

FIG. 4. **The N-terminal domain of human HGF inhibits angiogenesis *in vitro*.** HUVECs were cultured in three-dimensional collagen in the presence of 10 ng/ml FGF-2, $VEGF_{165}$, or HGF. Purified N-terminal polypeptide (1 μM) was added at the same time to some wells (*lower panel*). After 48 h, only the cells in the control culture were reorganized into cords and tubes (*upper panel*). In the presence of N, the tube assembly was blocked. Results shown are representative of three independent experiments.

stimulated by 10% FBS (Fig. 2*D*). As reported in Fig. 2*D*, N had no effect on the proliferation of hASMC induced with PDGF BB, or on the growth of TE 85 and DLD-1 cells in the presence of 10% FBS. In contrast, N inhibited the proliferation of NHEK and Capan-1 cells induced by HGF or FGF-2 (Fig. 2*E*). No inhibition was observed when these cells were stimulated with HGF or FGF-2 in the presence of kringles. Only K1 demonstrated an inhibitory effect (about 50%) toward Capan-1 cells at higher concentration (5 μM, data not shown). Taken together, our data demonstrate that the inhibitory activity of the HGF N-terminal domain is not strictly specific toward the endothelial cells. Nevertheless this activity is restricted to the cell types (presumably of epithelial or endothelial origin), which respond to the GAG-dependent growth factors.

Effect of Isolated HGF Domains on HUVEC Migration—To determine the effect of isolated recombinant HGF domains on endothelial cell migration, an essential component of the angiogenic response, we used a modified Boyden chamber assay. In this assay the cells seeded in the upper chamber of Transwell plates would migrate across the porous filter, if the chemoattractive stimulus is present in the lower chamber. In the preliminary experiments we determined that HGF had a relatively high chemotactic potential (4- to 6-fold stimulation over non-stimulated control), whereas FGF-2 was a less potent motogen (2.5-fold stimulation, data not shown). Therefore, we studied the effect of our recombinant proteins on the HGF-induced migration (Fig. 3*A*). Only isolated HGF N-terminal domain was capable of inhibiting the HUVEC chemotaxis toward HGF (more than 90% inhibition). Some kringles had a slight inhibitory effect, but this effect was not significant (Fig. 3*A*). In the migration assay, we also observed that the effect of recombinant N on HUVEC was not specific regarding HGF, as this polypeptide also inhibited the FGF-2 and $VEGF_{165}$-induced HUVEC migration (Fig. 3*B*).

Isolated HGF N-terminal Domain Inhibits Angiogenesis in Vitro—The results of two previous sets of experiments indicated that the HGF-derived kringles had no inhibitory activity, whereas the N-terminal domain appeared to be a potential anti-angiogenic molecule. To confirm the anti-angiogenic activity of N, we used a model known as "angiogenesis *in vitro*." In this model, the HUVECs were suspended in a three-dimensional gel composed of type I collagen and underwent a number of events leading to the formation of a network of capillary-like tubes. The model reproduces several steps of the angiogenesis such as motility, morphogenesis, and the production of lytic enzymes, which makes the penetration of the extracellular matrix possible (33).

When grown in a three-dimensional collagen gel in the presence of FGF-2, $VEGF_{165}$, or HGF, HUVECs rapidly underwent morphogenesis forming a network of cords and tubes. After 24 h, HUVECs showed a characteristic elongated phenotype and sprouting extensions. Some cells formed short structures made of several branched and associated elongated cells (data not shown). After 48 h, more cells were involved in structure formation, but some died (Fig. 4). After 72 h, virtually all the cells were dead. When 1 μM N was added to HUVECs grown in three-dimensional collagen, no formation of structures was observed, whatever the growth factor and the length of time tested (Fig. 4, shown for 48 h). In the presence of the HGF-derived kringles, the capillary-like structures formed normally (data not shown).

Recombinant HGF N-terminal Domain Prevents the Growth Factor Binding to HUVECs—Recombinant HGF N-terminal domain clearly antagonized the angiogenic response induced by at least three different cytokines. This inhibition could occur at several levels: (i) by inhibiting the interaction with binding sites on the cell surface; (ii) by inhibiting the receptor phosphorylation; and (iii) by inhibiting some signaling pathways downstream of the receptor activation. To clarify the molecular mechanism of N inhibitory activity, we undertook the displacement experiments with radiolabeled HGF, $VEGF_{165}$, and FGF-2 (Fig. 5).

The recombinant K1 of HGF, which had no effect on the HUVEC proliferation, migration, and morphogenesis, was not able to compete with HGF for binding to HUVECs (Fig. 5*A*). In contrast, N inhibited HGF, $VEGF_{165}$, and FGF-2 binding to HUVECs in a concentration-dependent manner (Fig. 5). In the three cases, the displacement kinetics was best described by a simple bimolecular reaction model. The K_d values, calculated using a weighted non-linear curve fitting algorithm implemented in the KELL package, were of 17.1 ± 10.74 nM, 27.69 ±

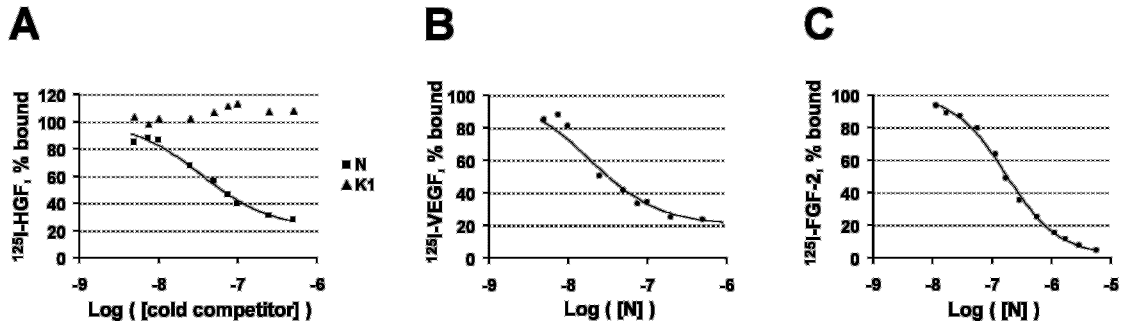

FIG. 5. **The N-terminal domain of human HGF inhibits the binding of growth factors to HUVECs.** Displacement analysis of 1.5 nM ^{125}I-labeled HGF (*A*), 1.2 nM ^{125}I-labeled VEGF$_{165}$ (*B*), and 1 nM ^{125}I-labeled FGF-2 (*C*) binding to HUVECs in the presence of unlabeled N or K1. Values on the *y*-axis are the mean values obtained from triplicate cultures. Results shown are representative of three or four experiments.

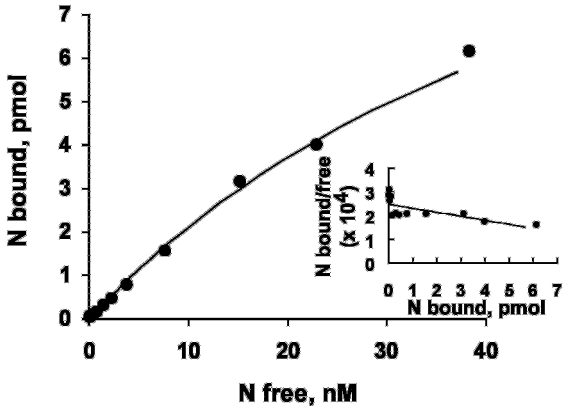

FIG. 6. **The recombinant N-terminal domain interacts with a single class of binding sites on the HUVEC surface.** ^{125}I-Labeled N was added to HUVECs (0.1–40 nM) and incubated for 6 h at 4 °C. The *inset* shows a Scatchard plot obtained using Ligand analysis. Results shown are representative of three experiments.

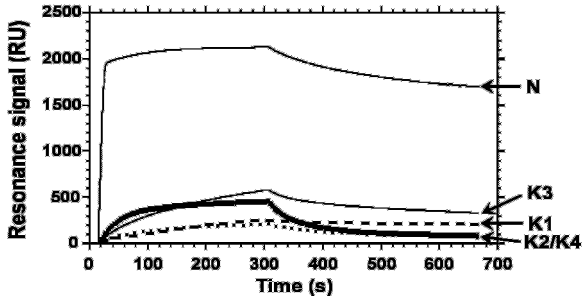

FIG. 7. **The N-terminal domain is the principal region involved in HGF-heparin interaction.** SPR analysis of the interaction of purified recombinant N (0.7 μM), K1 (9.5 μM) (*dashed line*), K2 (10.1 μM) (*bold line*), K3 (8.1 μM), or K4 (12.2 μM) (*thin dotted line*) with heparin immobilized on the surface of streptavidin-coated SA sensor chips. Results shown are representative of two experiments.

27.52 nM, and 68.16 ± 17.5 nM for HGF, VEGF$_{165}$, and FGF-2 displacement, respectively. These values were in good agreement with a K_d value of 67.9 ± 11.07 nM, obtained from the binding experiments between radiolabeled N and HUVECs. Scatchard analysis of the direct binding of N demonstrated the existence of a single class of binding sites (Fig. 6). Taken together these experiments indicated that N shares common binding sites with HGF, VEGF$_{165}$, and FGF-2 on HUVECs and that these sites are most probably of a low affinity nature.

SPR Analysis of the Interactions of HGF and Its Domains with Heparin and c-met—To gain insight into the molecular mechanism of the inhibitory activity of N, we compared the binding properties of this polypeptide with those of full-length HGF and of the four other isolated HGF α chain domains, using surface plasmon resonance (SPR) assays.

TABLE I
Kinetic parameters of the interaction between HGF α-chain domains and immobilized heparin

Bacterial expressed HGF α-chain domains were injected over biotinylated NF heparin immobilized on the surface of streptavidin-coated SA sensor chips. The binding curves were obtained at nine different analyte concentrations. The K'_d values were calculated from the ratio between k_{off} and k_{on}.

Analyte in solution	k_{on}	k_{off}	K'_d
	10^2 M^{-1} s^{-1}	$10^{-4}s^{-1}$	μM
N	1720 ± 100	2.58 ± 0.20	0.0015 ± 0.0002
K1	2.87 ± 0.16	4.64 ± 1.00	1.62 ± 0.36
K2	22.3 ± 3.1	40.6 ± 8.3	1.82 ± 0.45
K3	2.97 ± 0.68	9.09 ± 0.75	3.06 ± 0.74
K4	3.29 ± 0.39	19.8 ± 2.7	6.02 ± 1.13

We first studied the interaction of purified HGF domains with immobilized non-fractionated heparin. Representative results are shown in Fig. 7: all five HGF α-chain domains were able to bind heparin, but their binding characteristics presented major differences. The analysis of the binding curves indeed showed that N bound heparin with a 1000-fold higher affinity than any of the four kringles, mainly because its association rate constant k_{on} was much higher than that of the other HGF domains (Table I). N therefore clearly is the principal HGF domain involved in heparin binding.

In a parallel set of experiments, the purified HGF α-chain domains were injected over the c-met/Fc chimera immobilized on the surface of CM5 sensor chip. No binding could be observed for the HGF-derived kringles, whereas full-length HGF interacted strongly with c-met (data not shown). Although a slight binding of N to the immobilized c-met could be seen, the high background of nonspecific adhesion made it difficult to determine whether it was significant.

Therefore, we decided to undertake a whole new series of binding assays, in which the roles of the binding partners were swapped, *i.e.* we analyzed the binding of soluble c-met or heparin molecules to HGF domains immobilized on the surface of CM5 sensor chips. Representative examples of the results obtained are shown in Fig. 8. Only full-length HGF was able to interact with c-met (Fig. 8*A*), whereas no detectable binding could be evidenced for the five HGF α chain isolated subdomains (data shown only for N, Fig. 8*B*). The interaction of c-met with immobilized full-length HGF showed a complex kinetic behavior, which could be analyzed taking into account the dimeric (and therefore bivalent) nature of the c-met/Fc fusion. The kinetic parameters of the interaction were determined as follows: $k_{on}1 = 2.97\ (\pm 0.57) \times 10^4\ M^{-1}\ s^{-1}$; $k_{on}2 = 2.11\ (\pm 0.40) \times 10^{-3}\ RU^{-1}\ s^{-1}$; $k_{off}1 = 6.22\ (\pm 1.01) \times 10^{-3}\ s^{-1}$; $k_{off}2 = 4.31\ (\pm 0.50) \times 10^{-2}\ s^{-1}$. By analyzing the concentration

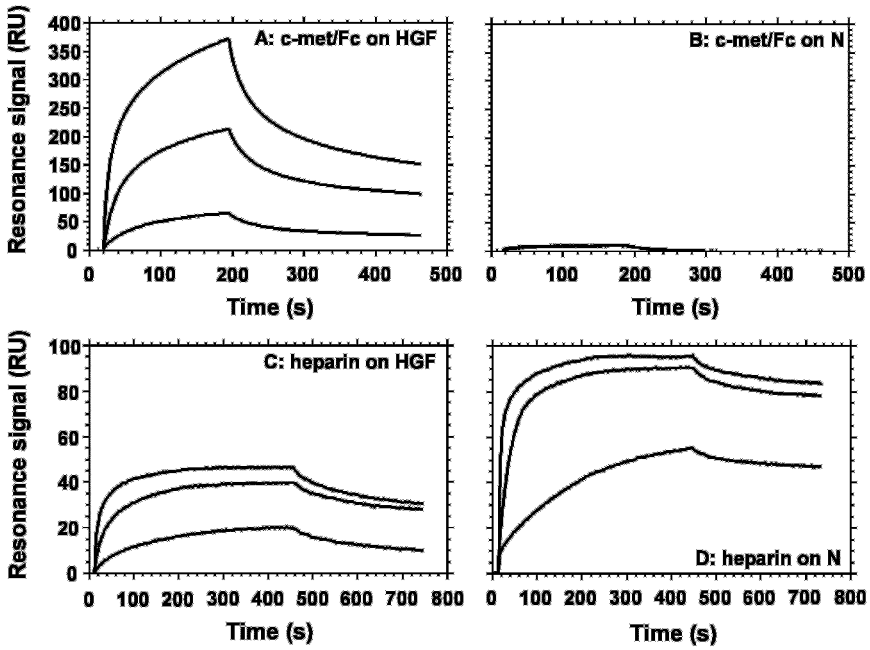

FIG. 8. **The N-terminal domain of human HGF binds to heparin but not to the c-met receptor *in vitro*.** SPR analysis of the interactions of HGF (*A* and *C*) and its N-terminal domain (*B* and *D*) with c-met/Fc chimera (12, 97, and 775 nM) (*A* and *B*) and non-fractionated heparin (2, 17, and 139 nM) (*C* and *D*). Results shown are representative of two experiments.

dependence of the steady-state responses, a K_d' of 50 (±4) nM could be determined for the interaction between c-met and HGF: this value considers the binding process globally without making any assumption on the mechanism of the interaction.

We finally studied the interaction with immobilized HGF and N of two different commercial heparin preparations: NF heparin and LMW heparin (data shown only for NF heparin, Fig. 8, *C* and *D*). The kinetic parameters of the interactions are shown in Table II: they were not significantly dependent on the amount of immobilized ligand (data not shown). Interestingly, NF heparin bound ~25 times better than LMW heparin, both to HGF and N (Table II): NF heparin showed both higher association rates, which could be due to the fact that its global electrostatic charge is higher (and therefore more favorable) than that of LMW heparin, and lower dissociation rates, which could be explained by the fact that NF heparin is statistically more multivalent (and therefore more avid) than LMW heparin. It should also be noted that the affinity of heparin for N is slightly stronger than that for full-length HGF (Table II): this 4-fold difference, only due to changes in k_{off}, could be linked to slight conformational modifications in the heparin binding site(s) of N, whether this domain is isolated or in the context of full-length HGF.

TABLE II
Kinetic parameters of the interaction between heparin and immobilized HGF or N domain

HGF and its isolated N terminal domain were immobilized on the surface of a CM5 sensor chip. NF heparin, and LMW heparin were used as analytes. The binding curves were obtained at twelve different analyte concentrations. The K_d' values were calculated from the ratio between k_{off} and k_{on}.

Immobilized ligand	Analyte in solution	k_{on}	k_{off}	K_d'
		$10^5\ M^{-1}\ s^{-1}$	$10^{-4}\ s^{-1}$	nM
HGF	NF heparin	11.0 ± 2.3	9.81 ± 0.91	0.89 ± 0.20
HGF	LMW heparin	1.52 ± 0.25	33.0 ± 4.8	21.7 ± 4.8
N	NF heparin	16.2 ± 3.2	3.49 ± 0.31	0.22 ± 0.05
N	LMW heparin	0.92 ± 0.13	5.30 ± 0.80	5.76 ± 1.19

DISCUSSION

HGF is a powerful endothelial cell mitogen, motogen, and morphogen (9). Abnormal HGF levels have been shown to contribute to the increased or impaired angiogenesis associated with several human cancers (34–37) and with some other pathological situations, such as diabetes (38), diabetic retinopathy (39), and arthritis and osteoarthritis (40). Therefore, HGF and its receptor represent very attractive targets for the development of new pro- or anti-angiogenic therapies. Indeed, several reports have demonstrated the effectiveness of HGF-based strategies in the promotion of therapeutic angiogenesis (38, 41, 42) or in the prevention of pathological angiogenesis (43).

Understanding the relationship between the structure and function of HGF could provide a way of creating potent HGF antagonists and agonists useful for the treatment of angiogenesis associated disorders. At present, the significance of the modular structure of HGF and the mode of interaction of HGF with the c-met receptor are not completely understood. Protein engineering experiments and x-ray crystallography analysis have shown that the c-met receptor and heparin binding regions were located within the α chain, and more precisely, within NK1 (15, 16, 18). NK1 was further identified as a partial c-met receptor agonist *in vivo* (44). Recent studies have demonstrated that K1 alone is sufficient to bind to and activate the c-met receptor (45). Interestingly, the addition of the following kringles to NK1 changed the biological activity of the resultant polypeptide. Thus, NK2, another naturally occurring HGF variant composed of N and the two first kringles, antagonized the HGF-induced cell growth *in vivo* but facilitated cell motility (46). Finally, NK4, an entire HGF α chain, has been shown to compete successfully with the native HGF for the binding to the receptor and inhibit the diverse biological responses to HGF, including the angiogenic response (47–49). These observations suggested that an anti-angiogenic activity could be located within the HGF kringle domains. This inhibitory activity could depend on the ability to displace HGF from its receptor, and this mechanism could be common with anti-angiogenic kringles of other origin.

To understand the mode of interaction of HGF with its receptor and establish the regions with antagonistic activity, we produced all five HGF α-chain domains as recombinant proteins and tested their ability to inhibit the angiogenic response induced in HUVECs. Our results demonstrated that none of the isolated HGF kringles was capable of inhibiting the endothelial cell proliferation, migration, and morphogenesis in a three-dimensional collagen gel. In contrast, the N-terminal domain was identified as a new anti-angiogenic polypeptide.

The inhibitory activity of N was not specific toward HGF, because N successfully inhibited the HUVEC proliferation, migration, and morphogenesis induced by other growth factors, such as FGF-2 and $VEGF_{165}$. Moreover, in contrast to the full-length HGF, the HGF N-terminal domain did not interact significantly with the c-met/Fc chimera *in vitro*. Therefore, the mechanism of anti-angiogenic activity of N was not dependent on the competitive binding to the HGF receptor.

SPR studies showed that none of the isolated domains of the α chain was capable to bind to the c-met receptor *in vitro*. This indicates that the c-met binding determinant in the native cytokine could involve several modules. Our results seem to be in disagreement with the findings that K1 is able to induce the c-met phosphorylation (45). Nevertheless, in the cited report, the authors showed that the c-met receptor activation in the presence of K1 was strongly dependent on the presence of heparin or heparan sulfate. The absence of K1 binding in our *in vitro* experiments using purified proteins could therefore be explained by the fact that heparan sulfate is required for the binding of K1 to the receptor *in vivo*.

We have demonstrated in this work that K1 and three other HGF kringles were able to bind heparin *in vitro*, albeit with a relatively low affinity. These results are in agreement with the recently published x-ray crystal structure of NK1-heparin complexes, which have shown that heparin is in contact with several amino acid residues in N and in K1 (18). The K_d calculated from our SPR experiments for the binding of different HGF kringles to heparin did not differ significantly between the kringles but were three orders of magnitude lower than that of N. From these data K2 does not seem to contribute in a particular way to the HGF interaction with heparin, in contrast with the conclusion drawn from earlier experiments with HGF deletion mutants (16).

The demonstration that N preserved the heparin binding activity of full-length HGF but did not bind the c-met receptor *in vitro* ruled out the possibility of contamination of the c-met/Fc preparations with cellular glycosaminoglycans (GAGs). Therefore, the HGF binding to c-met/Fc chimera observed in our SPR experiments is GAG-independent. Nevertheless, we obtained a K_d value that was substantially lower than that obtained in the earlier *in vivo* studies (nanomolar against picomolar order). This is consistent with the data showing that HGF is less efficient at inducing the receptor activation in the heparan sulfate-deficient cells (45). Taken together these results indicate that the cell surface GAGs could increase the affinity of HGF toward c-met.

Despite the progress in the understanding of the role of heparin and other GAGs in the growth factor receptor signaling, the mechanisms through which they regulate this process remain incompletely understood. GAGs are believed to be physiologically required co-receptors for a number of growth factors, by providing secondary binding sites that complement the interaction with the specific receptor and strengthen the adhesive forces (50). GAGs also promote dimerization/oligomerization of growth factors. This allows the monomeric ligands such as FGF to induce receptor dimerization, which is widely accepted as a prerequisite for the receptor activation. According to this model, a monomeric receptor remains inactive until the oligomerized ligand binds and oligomerizes the receptor, allowing autophosphorylation of receptor-associated kinases (51). Nevertheless, an increasing number of data suggest that GAGs do not act only by oligomerizing either ligand or receptor and that their role could be to induce the conformational changes in ligand and/or receptor (52, 53).

Our results suggest that the anti-angiogenic activity of N is dependent on its high heparin binding capacity. The displacement experiments with HUVECs showed that N acts most probably at the level of growth factor binding to the secondary binding sites, presented by cell surface GAGs. Interestingly, our results demonstrated that N inhibited more efficiently the binding of HGF and $VEGF_{165}$ than that of FGF-2. This is in good agreement with the available data on the structure of the heparin binding sites of the three growth factors. Thus, the structure of the 55-residue heparin binding domain of $VEGF_{165}$ is remarkably similar to the structure of the hairpin-loop region within N domain of HGF, which forms part of the putative heparin binding site (17, 54). On the contrary, the folding pattern of the FGF-2 heparin binding site is quite different from that of the two other growth factors (55). Previous studies had also indicated that the heparin sequence that binds FGF-2 differs from the one that binds HGF. Thus, 2-*O*-sulfates in iduronic acid, *N*-sulfates in glucosamine, and the carboxylate group in iduronic acid units of heparin are involved principally in the interaction with FGF-2, whereas 6-*O*-sulfates in glucosamine units seem to be of less importance (55–57). In contrast, 6-*O*-sulfates are the major determinants of the heparin-HGF interaction, with 2-*O*-sulfates playing minor role (18, 58). Similarly, the $VEGF_{165}$-heparin interaction involves principally the 6-*O*-sulfates and *N*-sulfates in glucosamine with a minor contribution of 2-*O*-sulfates in iduronic acid (59). Thus, our results are in agreement with the available data on the structural basis of the interaction of FGF-2, HGF, and $VEGF_{165}$ with sulfated polysaccharides.

N could also interfere with the pre-existing c-met/GAG interaction. Recent results suggest that the role of GAG in growth factor signaling is more complex than that predicted previously on the basis of ligand-GAG interaction alone. Thus, it has been shown that some growth factor receptors, including c-met, are themselves able to bind with high affinity to GAGs, which presumably could stabilize the pre-existing oligomeric receptor clusters (45, 60). Further elucidation of the molecular mechanism of N inhibitory action could contribute to the understanding of the physiological significance of the c-met/GAG interaction and to the design of new anti-angiogenic molecules targeting the GAGs involved in receptor tyrosine kinase signaling.

Acknowledgments—We are very grateful to Dr. Alain Chaffotte for the CD spectra of the HGF domains and to the maternity departments of the Lariboisière (Paris) and Jean Rostand (Ivry-sur-Seine) hospitals for providing umbilical cord specimens. We thank Dr. Pascale Briand for pGEM/HGF-TM construct and Dr. Janne L. Simonsen for pRI expression strain.

REFERENCES

1. Nakamura, T., Nishizawa, T., Hagiya, M., Seki, T., Shimonishi, M., Sugimura, A., Tashiro, K., and Shimizu, S. (1989) *Nature* **342,** 440–443
2. Stoker, M., Gherardi, E., Perryman, M., and Gray, J. (1987) *Nature* **327,** 239–242
3. Matsumoto, K., and Nakamura, T. (1997) *CIBA Found. Symp.* **212,** 198–214
4. Park, M., Dean, M., Kaul, K., Braun, M. J., Gonda, M. A., and Vande, W. G. (1987) *Proc. Natl. Acad. Sci. U. S. A.* **84,** 6379–6383
5. Bottaro, D. P., Rubin, J. S., Faletto, D. L., Chan, A. M., Kmiecik, T. E., Vande, W. G., and Aaronson, S. A. (1991) *Science* **251,** 802–804
6. Comoglio, P. M., and Trusolino, L. (2002) *J. Clin. Invest.* **109,** 857–862
7. Bussolino, F., Di Renzo, M. F., Ziche, M., Bocchietto, E., Olivero, M., Naldini, L., Gaudino, G., Tamagnone, L., Coffer, A., and Comoglio, P. M. (1992) *J. Cell Biol.* **119,** 629–641
8. Silvagno, F., Follenzi, A., Arese, M., Prat, M., Giraudo, E., Gaudino, G., Camussi, G., Comoglio, P. M., and Bussolino, F. (1995) *Arterioscler. Thromb. Vasc. Biol.* **15,** 1857–1865
9. Rosen, E. M., Lamszus, K., Laterra, J., Polverini, P. J., Rubin, J. S., and Goldberg, I. D. (1997) *CIBA Found. Symp.* **212,** 215–229
10. Van Belle, E., Witzenbichler, B., Chen, D., Silver, M., Chang, L., Schwall, R., and Isner, J. M. (1998) *Circulation* **97,** 381–390
11. Naldini, L., Tamagnone, L., Vigna, E., Sachs, M., Hartmann, G., Birchmeier, W., Daikuhara, Y., Tsubouchi, H., Blasi, F., and Comoglio, P. M. (1992) *EMBO J.* **11,** 4825–4833
12. Miyazawa, K., Shimomura, T., Kitamura, A., Kondo, J., Morimoto, Y., and Kitamura, N. (1993) *J. Biol. Chem.* **268,** 10024–10028
13. Hartmann, G., Naldini, L., Weidner, K. M., Sachs, M., Vigna, E., Comoglio, P. M., and Birchmeier, W. (1992) *Proc. Natl. Acad. Sci. U. S. A.* **89,** 11574–11578

14. Lokker, N. A., Mark, M. R., Luis, E. A., Bennett, G. L., Robbins, K. A., Baker, J. B., and Godowski, P. J. (1992) *EMBO J.* **11,** 2503–2510
15. Lokker, N. A., and Godowski, P. J. (1993) *J. Biol. Chem.* **268,** 17145–17150
16. Mizuno, K., Inoue, H., Hagiya, M., Shimizu, S., Nose, T., Shimohigashi, Y., and Nakamura, T. (1994) *J. Biol. Chem.* **269,** 1131–1136
17. Zhou, H., Mazzulla, M. J., Kaufman, J. D., Stahl, S. J., Wingfield, P. T., Rubin, J. S., Bottaro, D. P., and Byrd, R. A. (1998) *Structure* **6,** 109–116
18. Lietha, D., Chirgadze, D. Y., Mulloy, B., Blundell, T. L., and Gherardi, E. (2001) *EMBO J.* **20,** 5543–5555
19. Ikeo, K., Takahashi, K., and Gojobori, T. (1995) *J. Mol. Evol.* **40,** 331–336
20. O'Reilly, M. S., Holmgren, L., Shing, Y., Chen, C., Rosenthal, R. A., Moses, M., Lane, W. S., Cao, Y., Sage, E. H., and Folkman, J. (1994) *Cell* **79,** 315–328
21. Cao, Y., Ji, R. W., Davidson, D., Schaller, J., Marti, D., Sohndel, S., McCance, S. G., O'Reilly, M. S., Llinas, M., and Folkman, J. (1996) *J. Biol. Chem.* **271,** 29461–29467
22. Cao, Y., Chen, A., An, S. S., Ji, R. W., Davidson, D., and Llinas, M. (1997) *J. Biol. Chem.* **272,** 22924–22928
23. Lee, T. H., Rhim, T., and Kim, S. S. (1998) *J. Biol. Chem.* **273,** 28805–28812
24. Trieu, V. N., and Uckun, F. M. (1999) *Biochem. Biophys. Res. Commun.* **257,** 714–718
25. Nguyen, T. H., Pages, J. C., Farge, D., Briand, P., and Weber, A. (1998) *Hum. Gene Ther.* **9,** 2469–2479
26. Shima, N., Tsuda, E., Goto, M., Yano, K., Hayasaka, H., Ueda, M., and Higashio, K. (1994) *Biochem. Biophys. Res. Commun.* **200,** 808–815
27. Lokker, N. A., Presta, L. G., and Godowski, P. J. (1994) *Protein Eng.* **7,** 895–903
28. Bulteau, A. L., Verbeke, P., Petropoulos, I., Chaffotte, A. F., and Friguet, B. (2001) *J. Biol. Chem.* **276,** 45662–45668
29. Jaffe, E. A., Nachman, R. L., Becker, C. G., and Minick, C. R. (1973) *J. Clin. Invest.* **52,** 2745–2756
30. Yu, Q., and Toole, B. P. (1995) *BioTechniques* **19,** 122–129
31. Stahl, S. J., Wingfield, P. T., Kaufman, J. D., Pannell, L. K., Cioce, V., Sakata, H., Taylor, W. G., Rubin, J. S., and Bottaro, D. P. (1997) *Biochem. J.* **326,** 763–772
32. Kumar, R., Yoneda, J., Bucana, C. D., and Fidler, I. J. (1998) *Int. J. Oncol.* **12,** 749–757
33. Yang, S., Graham, J., Kahn, J. W., Schwartz, E. A., and Gerritsen, M. E. (1999) *Am. J. Pathol.* **155,** 887–895
34. Schmidt, N. O., Westphal, M., Hagel, C., Ergun, S., Stavrou, D., Rosen, E. M., and Lamszus, K. (1999) *Int. J. Cancer* **84,** 10–18
35. Wagatsuma, S., Konno, R., Sato, S., and Yajima, A. (1998) *Cancer* **82,** 520–530
36. Hendrix, M. J., Seftor, E. A., Seftor, R. E., Kirschmann, D. A., Gardner, L. M., Boldt, H. C., Meyer, M., Pe'er, J., and Folberg, R. (1998) *Am. J. Pathol.* **152,** 855–863
37. Horiguchi, N., Takayama, H., Toyoda, M., Otsuka, T., Fukusato, T., Merlino, G., Takagi, H., and Mori, M. (2002) *Oncogene* **21,** 1791–1799
38. Taniyama, Y., Morishita, R., Hiraoka, K., Aoki, M., Nakagami, H., Yamasaki, K., Matsumoto, K., Nakamura, T., Kaneda, Y., and Ogihara, T. (2001) *Circulation* **104,** 2344–2350
39. Cai, W., Rook, S. L., Jiang, Z. Y., Takahara, N., and Aiello, L. P. (2000) *Invest. Ophthalmol. Vis. Sci.* **41,** 1885–1893
40. Nagashima, M., Hasegawa, J., Kato, K., Yamazaki, J., Nishigai, K., Ishiwata, T., Asano, G., and Yoshino, S. (2001) *J. Rheumatol.* **28,** 1772–1778
41. Hayashi, K., Nakamura, S., Morishita, R., Moriguchi, A., Aoki, M., Matsumoto, K., Nakamura, T., Kaneda, Y., Sakai, N., and Ogihara, T. (2000) *Gene Ther.* **7,** 1664–1671
42. Taniyama, Y., Morishita, R., Aoki, M., Nakagami, H., Yamamoto, K., Yamazaki, K., Matsumoto, K., Nakamura, T., Kaneda, Y., and Ogihara, T. (2001) *Gene Ther.* **8,** 181–189
43. Abounader, R., Lal, B., Luddy, C., Koe, G., Davidson, B., Rosen, E. M., and Laterra, J. (2002) *FASEB J.* **16,** 108–110
44. Jakubczak, J. L., LaRochelle, W. J., and Merlino, G. (1998) *Mol. Cell Biol.* **18,** 1275–1283
45. Rubin, J. S., Day, R. M., Breckenridge, D., Atabey, N., Taylor, W. G., Stahl, S. J., Wingfield, P. T., Kaufman, J. D., Schwall, R., and Bottaro, D. P. (2001) *J. Biol. Chem.* **276,** 32977–32983
46. Otsuka, T., Jakubczak, J., Vieira, W., Bottaro, D. P., Breckenridge, D., LaRochelle, W. J., and Merlino, G. (2000) *Mol. Cell Biol.* **20,** 2055–2065
47. Date, K., Matsumoto, K., Shimura, H., Tanaka, M., and Nakamura, T. (1997) *FEBS Lett.* **420,** 1–6
48. Jiang, W. G., Hiscox, S. E., Parr, C., Martin, T. A., Matsumoto, K., Nakamura, T., and Mansel, R. E. (1999) *Clin. Cancer Res.* **5,** 3695–3703
49. Kuba, K., Matsumoto, K., Date, K., Shimura, H., Tanaka, M., and Nakamura, T. (2000) *Cancer Res.* **60,** 6737–6743
50. Carey, D. J. (1997) *Biochem. J.* **327,** 1–16
51. Schlessinger, J. (2000) *Cell* **103,** 211–225
52. Park, P. W., Reizes, O., and Bernfield, M. (2000) *J. Biol. Chem.* **275,** 29923–29926
53. Lyon, M., Deakin, J. A., and Gallagher, J. T. (2002) *J. Biol. Chem.* **277,** 1040–1046
54. Fairbrother, W. J., Champe, M. A., Christinger, H. W., Keyt, B. A., and Starovasnik, M. A. (1998) *Structure* **6,** 637–648
55. Faham, S., Hileman, R. E., Fromm, J. R., Linhardt, R. J., and Rees, D. C. (1996) *Science* **271,** 1116–1120
56. Guimond, S. E., and Turnbull, J. E. (1999) *Curr. Biol.* **9,** 1343–1346
57. Pellegrini, L., Burke, D. F., von Delft, F., Mulloy, B., and Blundell, T. L. (2000) *Nature* **407,** 1029–1034
58. Lyon, M., Deakin, J. A., Rahmoune, H., Fernig, D. G., Nakamura, T., and Gallagher, J. T. (1998) *J. Biol. Chem.* **273,** 271–278
59. Ono, K., Hattori, H., Takeshita, S., Kurita, A., and Ishihara, M. (1999) *Glycobiology* **9,** 705–711
60. Schlessinger, J., Plotnikov, A. N., Ibrahimi, O. A., Eliseenkova, A. V., Yeh, B. K., Yayon, A., Linhardt, R. J., and Mohammadi, M. (2000) *Mol. Cell* **6,** 743–750